Continuous laser welding with spatial beam oscillation of dissimilar thin sheet materials (Al-Cu and Cu-Al): Process optimization and characterization

Continuous laser welding with spatial beam oscillation of dissimilar thin sheet materials (Al-Cu and Cu-Al): Process optimization and characterization

Vincenzo Dimatteo*, Alessandro Ascari, Alessandro Fortunato

University of Bologna, Viale del Risorgimento, 2, Bologna, 40136, Italy

A B S T R A C T

Continuous laser welding with spatial beam oscillation was investigated as a method of joining combinations of thin copper and aluminum sheets. Welding of these materials is required for manufacturing of electronic components due to their physical properties. Welding of dissimilar metals such as Al-Cu with conventional manufacturing techniques is difficult due to unavoidable formation of brittle intermetallic compounds, which reduce both the mechanical and electrical properties of the joint. The aim of this work was to understand how process parameters such as laser power, welding speed and wobbling amplitude affected the weld seam, making it possible to determine which parameters were of greatest influence on the mechanical and electrical properties of the resulting joint. Both the width and penetration of the weld seam were strongly correlated to the wobbling amplitude. The ultimate tensile strength of both configurations (Al-Cu and Cu-Al) was as high as 100 kgf with optimized process parameters. Micro-hardness tests showed an increase in hardness near the molten area. The temperatures attained during welding were approximately 40 °C at 10 mm from the weld seam. Low electrical contact resistance and high tensile strengths were obtained with the same parameters.

Keywords:
Continuous laser welding
Spatial beam oscillation
Thin sheet materials
Aluminium and copper
Dissimilar welding

1. Introduction

Over recent years, most governments have enacted increasingly stringent laws on air pollution. In particular, the European Union set a target of 95 g CO_2/km for the average emissions of new cars produced from 2020 onwards [1]. Due to these emission limits, the demand for electric vehicles (EVs) and hybrid-electric vehicles (HEVs) has increased. One of the challenges that must be faced with these vehicles is the design of a battery system able to provide high power density and minimal electrical losses. Lithium-ion batteries are key components in the pursuit of high performance energy storage for electric vehicles. Their main advantages compared to other battery types such as NiMH cells are good volumetric power and energy density, and high open-circuit voltage [2]. A battery pack consists of hundreds of cells, with electrode current collectors in aluminum (cathode) or copper (anode), which are connected in series and parallel. A reliable weld seam with good mechanical characteristics and low electrical resistance is therefore required.

Aluminum (Al) and copper (Cu) are widely used as electrical connectors in various applications due to their good corrosion resistance and electrical conductivity [3]. For years, both materials have been considered very difficult to weld; however, growing demand for aluminum and copper components poses new challenges. Fusion welding of Al and Cu is difficult to achieve due to their significantly different chemical composition and physical properties. The most important issue in welding Al and Cu is that while mutual solubility between the two metals occurs in the liquid state, brittle intermetallic compounds (IMC) form after solidification resulting in degradation of the weld properties [4]. By analyzing the Al-Cu equilibrium phase diagram it is possible to find different intermetallic compounds. The intermetallic phases have higher brittleness, lower mechanical strength, and higher electrical resistivity than the base materials [5], which leads to deterioration of both the mechanical and electrical properties of the weld joint. These brittle intermetallic compounds can act as crack initiation points due to the significant difference in melting temperature, thermal conductivity and thermal expansion between the base metals [6]. It is clear that to obtain a reliable joint, the formation of intermetallic compounds must be avoided. Many works have attempted to apply conventional welding technology such as friction stir welding but have not produced defect-free weld seams [7]. Conventional welding processes are also characterized by low flexibility and repeatability. The main technological requirement is therefore to achieve a short cycle

time and high energy density over a small area, as well as non-equilibrium temperature gradients to avoid the formation of intermetallic compounds. Laser beam welding (LBW) is well suited to these requirements. Its high energy density makes it possible to melt dissimilar metals with different thermal conductivities, while the low heat input results in rapid heating and cooling, which translates into a unique advantage in terms of welding dissimilar metals [8].

Laser beam welding is characterized by numerous advantages such as high power density focused into a small spot, good weld quality, good precision, ease of automation and flexibility in comparison with conventional welding technology [9]. Over the last few decades, different laser sources have been developed for various applications including welding, cutting and cladding. Particular attention has been paid towards high-brilliance laser sources that represent a key tool for industrial manufacturing in terms of wavelength and available power in continuous wave [10]. Welding of dissimilar metals with a CW laser involves significant mixing of the two materials, with large cracks along the weld seam being a significant problem [11]. Many authors suggest the use of spatial beam oscillation to weld dissimilar metals and to improve joint quality. Uniform mixing of the two materials in the weld seam has been demonstrated using a single-mode fiber laser and spatial beam oscillation [12]. It has been shown that the wobbling mode allows large joint widths to be obtained and low penetration into the underlying sheet [11] providing good mechanical properties. The aim is to achieve a weld seam with large width at the interface for good mechanical strength and partial penetration into the underlying material to avoid excessive mixing. Solchenbach et al. [13] demonstrated that lowest electrical resistance and highest strength can be achieved with the same parameter set. Most studies performed to date focus on how the wobbling parameters affect the weld seam and intermetallic compounds for sheets with thickness in the order of one millimeter in different combinations using high power fiber (2–3 kW) lasers [12,14]. In this study, a single-mode fiber laser with maximum output power of 1 kW has therefore been used to weld thin aluminum and copper sheets in both Al-Cu and Cu-Al configurations with the purpose of finding an appropriate parameter window and characteriz ing the process with optimized parameters.

2. Materials and methods

Experiments were conducted by varying the laser power, welding speed and beam wobbling amplitude. Welding experiments were repeated twice for each parameter combination. In the first phase, the objective of the study was to investigate how process parameters influenced the morphology of the weld seam including the surface width, width at the interface and penetration depth. In order to monitor the temperature during welding, thermocouples were assembled on the sheets. Afterwards, the welds with partial penetration were mechanically characterized via tensile and micro-hardness tests, while electrical measurements were also performed. Finally, double weld seams were produced based on the best conditions and were tested to improve joint properties.

Table 1
Thermocouple specifications.

Thermocouples	
Parameter	Value
Type	K
Thickness	1 [mm]
Sampling time	2 [s]
Sampling rate	1 [ms]

The materials used for the investigation included EN-AW 1050 aluminum alloy sheets (99.5% Al) of thickness 0.45 mm and pure C1020-HO copper sheets (99.9% Cu) of thickness 0.3 mm. A thin layer of electroplated nickel (2.5 µm) was employed to increase beam absorption when the copper sheet was on upper side. The size of the samples was 45 mm wide and 70 mm long, with welding performed in an overlap configuration with an overlap of 15 mm. A clamping system was designed to guarantee correct adhesion between the sheets during welding. Four thermocouples were positioned on the top of both sheets at a distance of 10 mm from the welding area to monitor the maximum temperature attained during the process, as shown in Fig. 1(b). Thermocouple specifications are reported in Table 1. The same specimens were used for tensile tests. Fig. 1(a) shows a representation of the laser setup. Samples were cleaned with an acetone solution before welding.

A single-mode IPG YLR 1000-SM fiber laser with wavelength of 1064 nm and maximum power of 1000 W was used for all experiments in combination with a galvanometric scanning head equipped with an F-Theta lens. The laser beam was orthogonal to the specimens with the laser beam focused on the surface of the top layer for both configurations. No shielding gas was used during welding experiments and no back-reflection phenomenon was detected. Laser source and optics specifications are shown in Table 2.

The aim of the study was to characterize the welding process with a given circular spatial beam oscillation and feed rate. The wobbling strategy was implemented by programming the galvanometric scanning

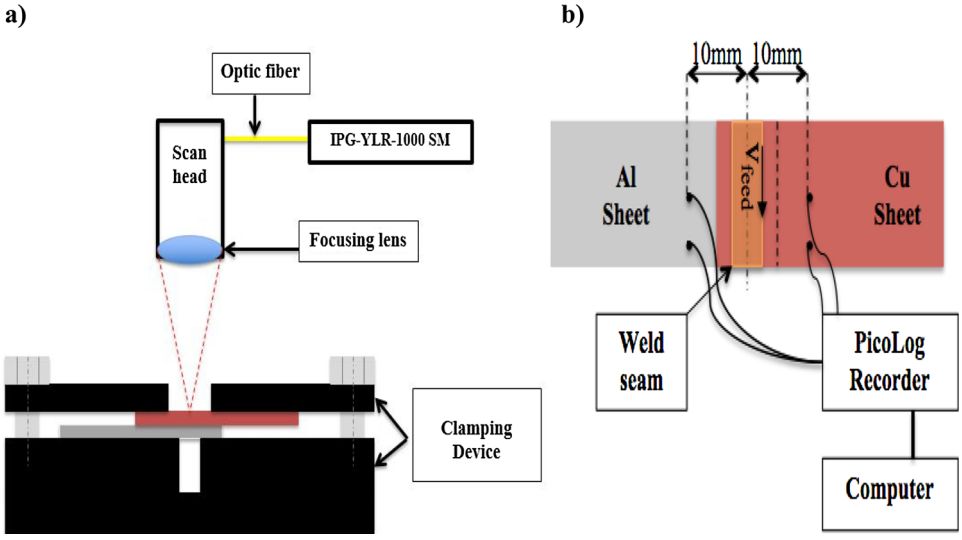

Fig. 1. Laser set up (a) and thermocouples positioning (b).

Table 2
Laser source and optics specifications.

Laser source		Optical path	
Specification	Value	Specification	Value
Emission Wavelength	1064 nm	Collimation length	100 mm
Operating mode	CW	Focal length	420 mm
Emission power	1000 W	Fiber core diameter	14 μm
BPP	0.4 mm*mrad	Focal spot diameter	60 μm

head to achieve a laser path resulting from the super positioning of circular and linear motion, as shown in Fig. 2(top).

The beam was made to rotate along a circular path with a diameter equal to the wobbling width A and a tangential speed V_t. The center of the circular path was moved along the welding direction at a constant speed V_f, so that two subsequent revolutions achieved a fixed percentage overlap. The mathematical formulas governing this combined motion are given in Eq. (1).

$$\begin{cases} x(t) = \frac{A}{2}\cos\left(\frac{2V_t}{A}t\right) + V_f t \\ y(t) = \frac{A}{2}\sin\left(\frac{2V_t}{A}t\right) \end{cases} \quad (1)$$

Based on these considerations, the actual beam path was a cycloid similar to that shown in Fig. 2(bottom). The equipment used in the experimental activity was programmed in terms of wobbling amplitude (A), overlap and tangential speed (V_t). The wobbling frequency (f) and welding speed (V_f) can be calculated with Eqs. (2) and (3).

$$f = \frac{V_t}{\pi A} \quad (2)$$

$$V_f = f\left(A - \left(\frac{A \cdot Overlap}{100}\right)\right) \quad (3)$$

The linear welding speed and scanning frequency were then calculated by taking into account these equations, the laser beam velocity (V_t) and wobbling amplitude. Values are reported in Tables 3 and 4.

Preliminary studies were conducted to establish a feasible range of test parameters. A Design of Experiment was then carried out to conduct experiments. Table 5 shows the parameters used. For each set of parameters, welds of 45 mm length were generated.

Cross sections were prepared by mounting the samples in resin and polishing to a grit size of 800 followed by 0.5 μm alumina in suspension. Microscopy was performed with a ZEISS Axio Vert.A1M with no etchant to identify the weld seam geometry.

Shear strength tests were performed at room temperature with an INSTRON 8033 tensile testing machine at a crosshead speed of 0.025 mm/s. It must be noted that samples used for tensile tests were not standardized since the aim was to qualitatively evaluate the effectiveness of the joint. To guarantee a coaxial load, samples were thickened during assembly in the press. Tests were performed to obtain the ultimate tensile load and point at which fracture took place. For each combination of parameters, two specimens were welded and the average values of maximum breaking load was calculated. Vickers

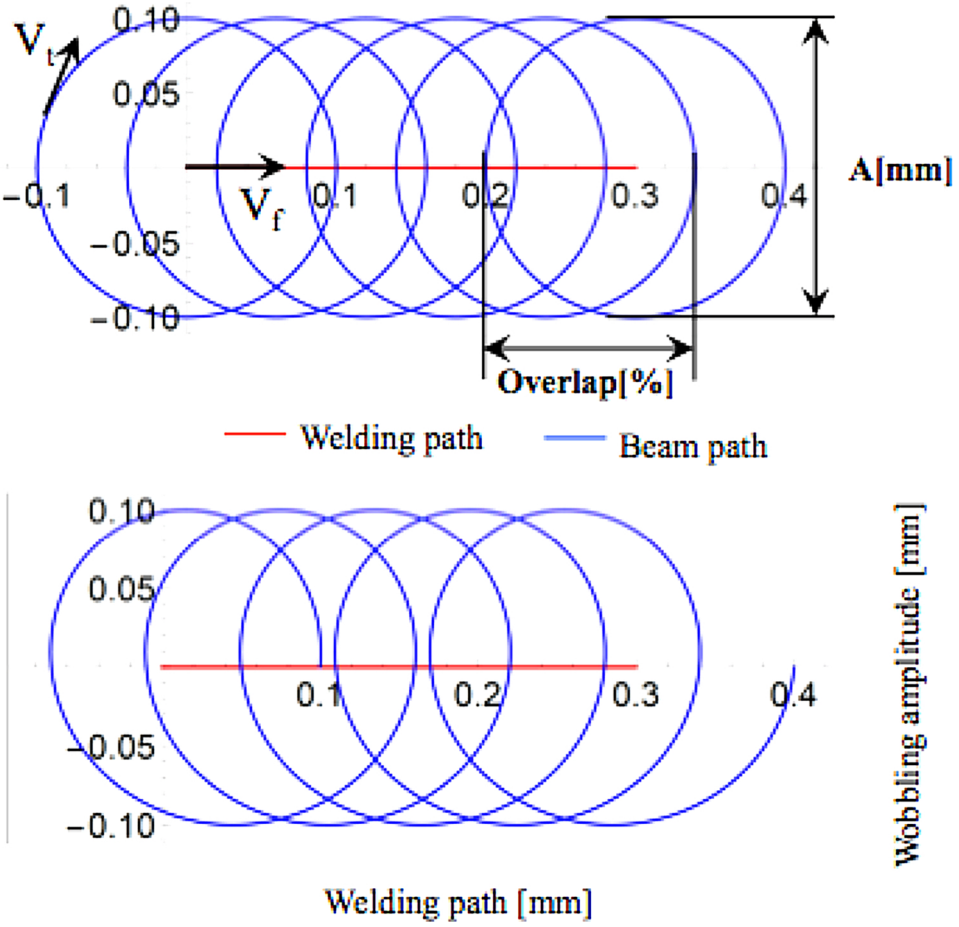

Fig. 2. Schematic of wobbling strategy and feed.

		Laser beam velocity (Vt)					
		Al-Cu			Cu-Al		
Wobbling amplitude	**Overlap**	**600** [mm/s]	**700** [mm/s]	**800** [mm/s]	**400** [mm/s]	**500** [mm/s]	**600** [mm/s]
0.2-0.5-0.7 [mm]	30 [%]	133 [mm/s]	156 [mm/s]	178 [mm/s]	89 [mm/s]	111 [mm/s]	134 [mm/s]

Table 4
Scanning frequency calculated as a function of laser beam velocity (V_t) and wobbling amplitude.

			Wobbling amplitude		
			0.2 [mm]	0.5 [mm]	0.7 [mm]
Laser beam velocity (Vt)	**Al-Cu**	**600** [mm/s]	955[Hz]	382[Hz]	272[Hz]
		700 [mm/s]	1114[Hz]	445[Hz]	318[Hz]
		800 [mm/s]	1273[Hz]	510[Hz]	363[Hz]
	Cu-Al	**400** [mm/s]	637[Hz]	254[Hz]	182[Hz]
		500 [mm/s]	796[Hz]	318[Hz]	227[Hz]
		600 [mm/s]	955[Hz]	382[Hz]	272[Hz]

resistance of the base materials by using a resistance factor k [**17**]. For dissimilar material connections, the resistance factor k can be calculated with the following equation:

$$k = \frac{2*Rx}{Ral + Rcu} \quad (4)$$

If the resistance factor is 1, the contact resistance (Rx) is the same as the base material resistance, in this case aluminum and copper [17].

3. Results and discussion

3.1. Optical microscopy

Microscope images of typical results obtained with aluminum as the

Table 5
Welding parameters.

Configuration	Laser Power [W]	Welding linear speed [mm/s]	Wobbling amplitude [mm]	Scanning frequency [Hz]
Al-Cu	600-700-800	133-156-178	0.2-0.5-0.7	272 - 1273
Cu-Al	800-900-1000	89-111-134	0.2-0.5-0.7	182 - 955

micro-hardness tests were carried out with a load of 100 g for 20 s.

For electrical measurements, a four-point probe measurement technique was applied to determine the contact resistance. The set-up can be seen in Fig. 3. Measurements were carried out with a HIOKI RM3548 multimeter by applying a current of 1 A, thus measuring the resistance of the joints. The contact resistance was compared to the

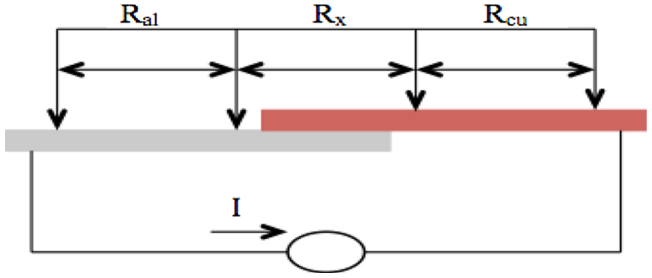

Fig. 3. Test set-up of four-point measurement.

upper layer are shown in Fig. 4. Three different conditions were achieved: under-welding, good welding and over-welding. Under-welding (Fig. 4(a)) was recorded at the highest trace width (0.7 mm), highest welding velocity and power levels of 600 W and 700 W. In these conditions, heat transferred from the laser beam to the material was clearly insufficient to effectively melt the upper material and subsequently mix with the lower layer. Good welding conditions (Fig. 4(b)) were obtained over a wide parameter range for all trace widths. It can be noted that each trace width had an optimum set of parameters. When the upper material did not penetrate completely in the lower material there was no excessive mixing and pores did not form. Where the power density was too high, excessive mixing of materials occurred with excessive pore formation. This last condition is to be avoided due to the elevated presence of defects and dripping that may compromise the mechanical integrity of the joint.

Once cross-sections were obtained, it was possible to measure the characteristic geometric quantities of each weld bead. The weld width was measured at the interface between the two sheets, while the penetration depth was taken as the depth into the lower sheet from the

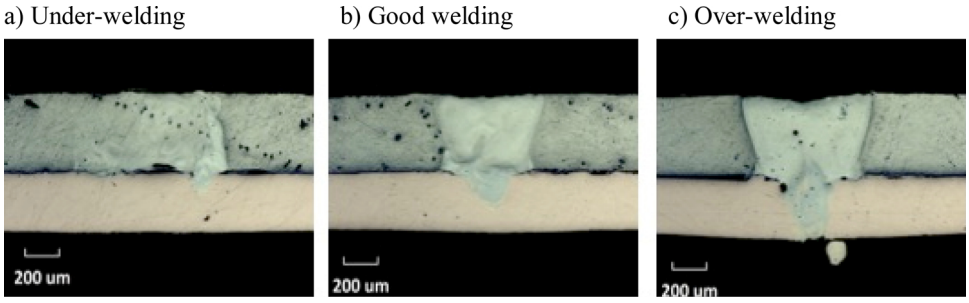

Fig. 4. Cross sections of Al-Cu configuration.

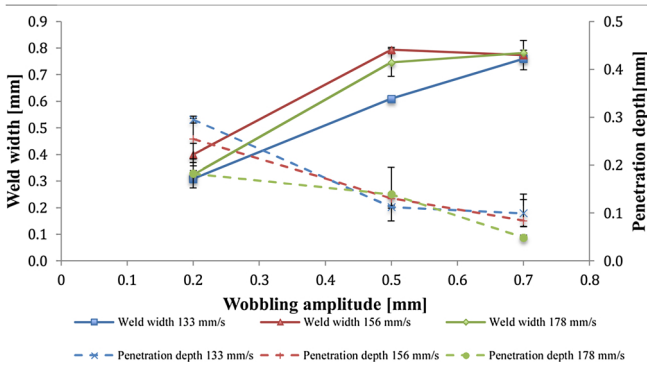

Fig. 5. Weld width and penetration depth as a function of wobbling amplitude for a laser power of 700 W.

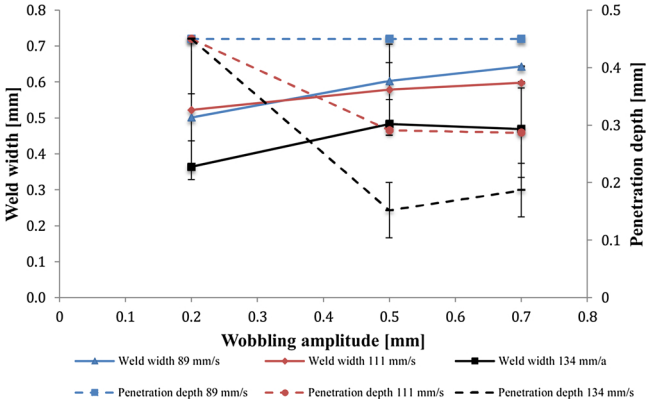

Fig. 7. Weld width and penetration depth as a function of wobbling amplitude for a laser power of 800 W.

interface. Two measurements were performed for each point. Average values and standard deviations for each parameter set are shown in Figs. 5 and 7.

The correlation between the weld width, penetration depth and wobbling amplitude at a laser power of 700 W is shown in Fig. 5 as a function of welding speed. Weld width increases linearly with wobbling amplitude from 0.2 mm to 0.5 mm. An increase in wobbling amplitude does not increase the weld width at the highest tested velocity. As can be seen, the weld width is about 0.7 mm at 156 mm/s and 178 mm/s for both wobbling amplitudes of 0.5 and 0.7 mm. At lower velocity, the weld width instead shows dependence on the wobbling amplitude. It is of interest to note that the weld width strongly depends on the wobbling amplitude; higher values such as 0.5 mm and 0.7 mm stabilize the process for different welding speeds. This is in contrast with the penetration depth, which decreases with increasing wobbling amplitude over the range 0.2 mm to 0.5 mm. For a wobbling amplitude of 0.2 mm and welding speed of 133 mm/s, over-welding conditions were recorded. By analyzing the penetration depth, it can be seen that this parameter reaches a value of about of 0.18 mm. At a wobbling amplitude of 0.7 mm, a penetration depth of 0.05 mm was obtained with a welding speed of 178 mm/s. The same results were obtained with other power levels considered in the experiment. It is clear that to achieve good welding and therefore partial penetration into the lower sheet, higher wobbling amplitude should be used since this strongly influences the weld seam geometry.

The same considerations can be made for the configuration in which the copper layer was placed above the aluminum layer. In this case, two different conditions were achieved, as reported in Fig. 6. With copper as the upper layer, the welding process was less stable and it was difficult to obtain a good joint free from defects such as pores. From microscopic analysis it is evident that the melted copper sinks in the lower aluminum layer due to its higher density, thus obtaining complete penetration in most experiments. As such, welding was achieved with all tested process parameters. Partial penetration (Fig. 6(a)) was achieved with a wobbling amplitude between 0.5 mm and 0.7 mm and a laser power of 800 W and 900 W. By increasing the laser power with the same amplitude, complete penetration and cutting was obtained. Full penetration, as can see in Fig. 6(b), is characterized by a large amount of defects that compromise the mechanical properties of the joint. A wobbling amplitude of 0.2 mm was not the best option to achieve a reliable joint based on optical analysis.

The correlation between weld width, penetration depth and wobbling amplitude at a laser power of 800 W and different welding speeds is shown in Fig. 7. Increasing the wobbling amplitude resulted in constant weld width with welding speeds of 111 mm/s and 134 mm/s. With a welding speed of 89 mm/s, the weld width increased linearly with wobbling amplitude up to a value of 0.7 mm. As expected, lower values of weld width were obtained with the highest welding speed at constant wobbling amplitude. In contrast, the penetration depth was affected by the wobbling amplitude since the penetration depth decreased with increasing wobbling amplitude. For a wobbling amplitude of 0.2 mm, full penetration was achieved at all welding speeds. A welding speed of 89 mm/s was not considered the best option since it did not obtain partial penetration. The lowest values of penetration depth were obtained with the highest welding speed at 0.5 mm and 0.7 mm wobbling amplitude. It can therefore be concluded that increasing the wobbling range to 0.5 mm does not produce benefits in terms of geometric characteristics since the weld width and penetration depth remain mostly constant at high velocity.

3.2. *Tensile shear tests*

After metallographic preparation and optical microscopy, tensile shear tests were performed. As mentioned above, tensile tests were performed for samples obtaining partial penetration. The aim was to perform a qualitative analysis of the joint and measure the maximum breaking load. The optimal parameters chosen for tensile tests are

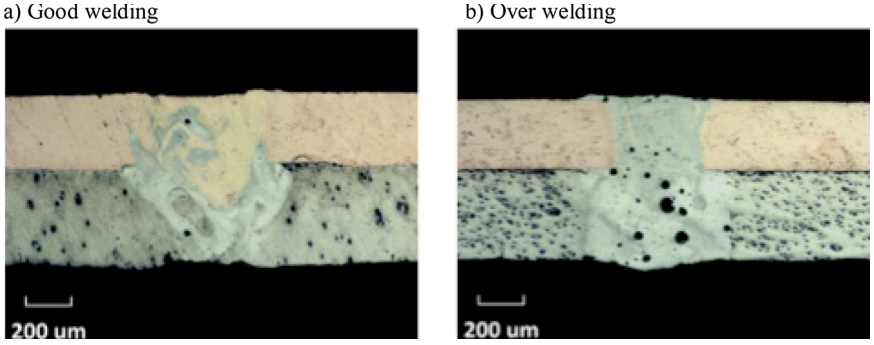

Fig. 6. Cross section of Cu-Al configuration.

Table 6
Optimal conditions used for tensile tests.

Configuration	Name	Power [W]	Welding speed [mm/s]	Wobbling amplitude [mm]	Weld width [mm]	Penetration depth [mm]
Al-Cu	A	600	156	0.2	0.30	0.19
	B	600	156	0.5	0.60	0.10
	C	800	134	0.7	0.82	0.17
Cu-Al	D	800	89	0.2	0.50	0.45
	E	900	134	0.5	0.60	0.40
	F	800	134	0.7	0.47	0.187

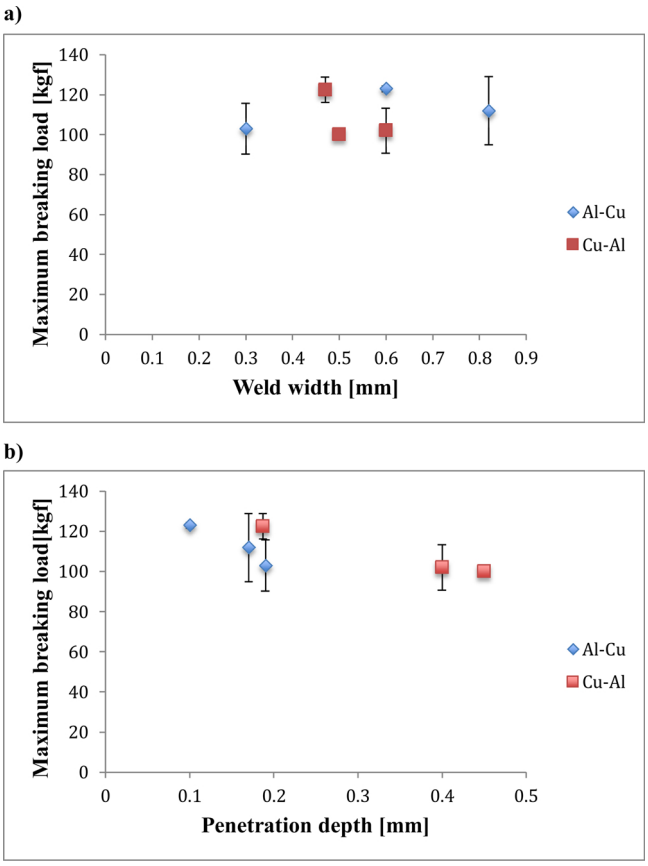

Fig. 8. Maximum breaking load as a function of weld width (a) and penetration depth (b).

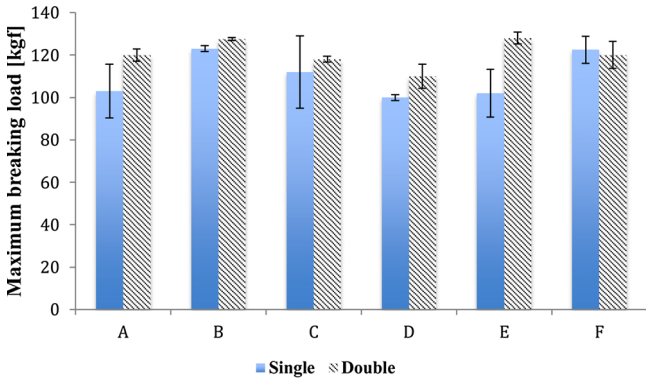

Fig. 9. Maximum breaking load of a single and double weld seams.

summarized in Table 6. In order to reduce the number of tests, only a few conditions were chosen, in particular one sample for each amplitude of wobbling. Two tests were carried out and the average was calculated.

Fig. 8(a) reports the maximum breaking load as a function of weld width for both configurations. With aluminum as the upper layer, the maximum breaking load was 123 kgf, with a weld width of 0.6 mm. With a weld width of 0.3 mm, the maximum breaking load was instead 103 kgf, while with a weld width of 0.82 mm, the load was 112 kgf. With copper as the upper layer, the maximum breaking load was achieved with a weld width of 0.47 mm. Further increases in weld width led to worse performance. Fig. 8(b) presents maximum breaking loads as a function of penetration depth. It is clear that as the penetration depth increases the maximum breaking load decreases for both configurations. Maximum values were obtained with penetration depths of 0.1 mm (Al-Cu) and 0.187 mm (Cu-Al).

After an initial phase in which the properties of single weld beads were assessed, the possibility of performing a double weld seam was assessed with the aim of improving the mechanical performance. Results obtained with a double weld seam are shown in Fig. 9. The double seam increases the mechanical strength by about 20% in all cases except for samples C and F, where the wobbling amplitude was 0.7 mm. It can be concluded that the double weld seam does not provide benefits with high amplitude wobbling since there is a greater probability of having larger molten and heat-affected zones, and therefore greater chance of finding defects that can compromise the mechanical properties. Finally, fracture mechanisms were analyzed. It was found that with an aluminum upper layer, fracture took place within the base material, indicating that the weld seam was stronger than the materials in both single and double-bead configurations. With copper as the upper layer, material breakage took place at the weld seam. Fracture near the weld seam could be due to the formation of Al-richer intermetallic compounds [15]. Further studies will be carried out to characterize intermetallic compounds formation.

3.3. Micro-hardness results

Micro-hardness tests were carried out on weld cross sections with 100 gf load force and 20 s dwell time. Indentations were performed longitudinally on both sheets in the fusion zone (FZ) at intervals of 300 μm. Starting from the central axis of the weld seam, five indentations were carried out; one at the axis and two each on the right- and left-hand sides. The hardness profiles obtained for both configurations are shown in Fig. 10. In (Fig. 10(a)) the hardness profile corresponding to specimen B with a wobbling amplitude of 0.5 mm is presented. It is interesting to observe how maximum hardness was obtained near the fusion zone in two different areas matching the extremes of the trace where the laser energy per unit length was maximum. It seems that with only one trace two weld seams were generated. The hardness of the base materials was 26 HV (Al) and 60 HV (Cu), while the maximum value in the fused zone was 190 HV. The aforementioned phenomenon was not observed in the Cu-Al configuration, presented in (Fig. 10(b)). A peak of 280 HV was obtained in the fusion zone close to the copper

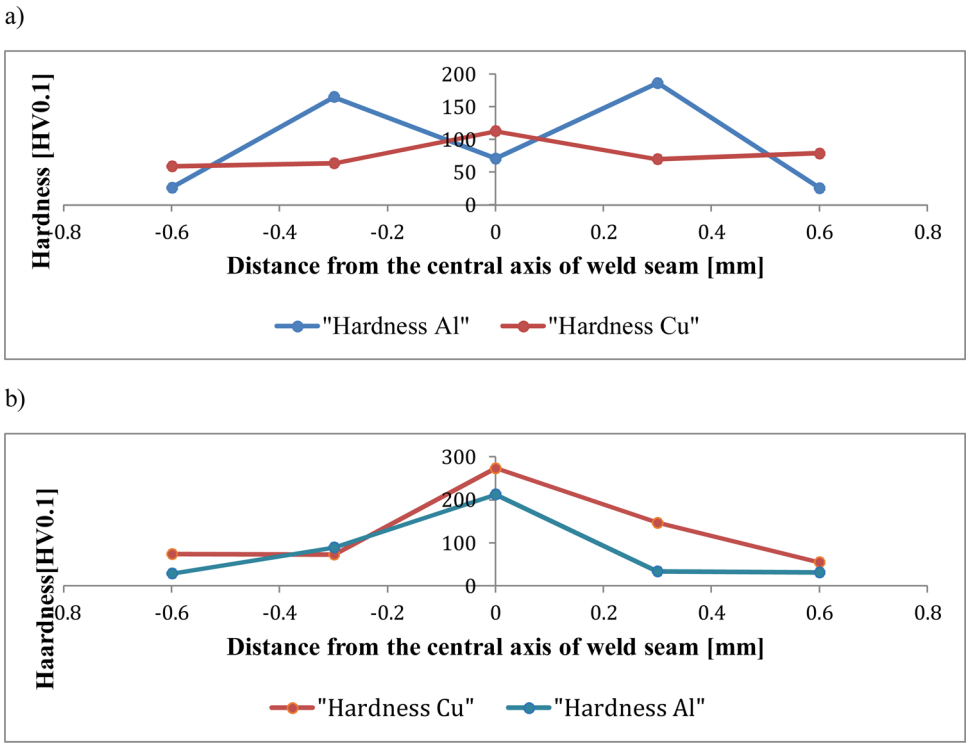

Fig. 10. Hardness curves obtained in Al-Cu (a) and Cu-Al (b) configurations.

sheet. By comparing the mechanical results and the hardness values, it can be deduced that hardness values of up to 300 HV have a negative influence on mechanical properties. Specifically, by analyzing the tensile test curves it can be noted that breakage is more fragile for the Cu-Al configuration than for the Al-Cu configuration. Further SEM analysis will be performed to characterize intermetallic compounds.

3.4. Temperature profile

During battery cell assembly, the primary application of this type of weld, it is important not to reach high temperatures to avoid melting the polymeric casing that surrounds the individual cells. Maximum measured temperatures are shown in Fig. 11. For the Al-Cu configuration, namely specimens A, B and C, maximum temperatures were about 28 °C in the case of a single weld seam. There is no substantial difference between the various values since the welding speed was not changed significantly and the wobbling amplitude did not seem to influence the result. With a double weld seam, the temperatures reach a value of about 33 °C. For the Cu-Al configuration, specimens D, E and F, temperatures were about of 32 °C in the case of single weld seams and about 40 °C with a double weld seem. The power densities and welding speeds used in this work therefore produce reliable joints with low thermal stress. The most stressed point was in correspondence with the central weld area on the sheet irradiated by the laser beam. The temperatures attained, however, were low compared to conventional welding technologies.

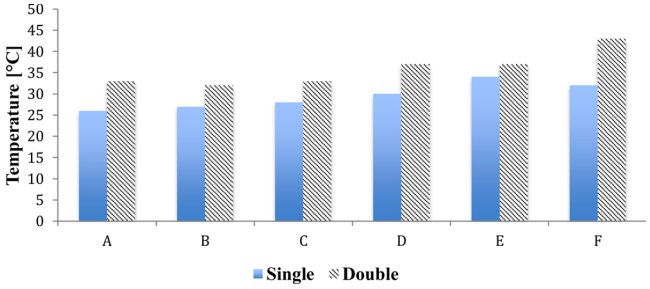

Fig. 11. Maximum recorded temperatures.

3.5. Electrical contact resistance

The measured resistance factor, k, of specimens is reported in Fig. 12. The resistance factor oscillates around unity, confirming that the weld seam has good electrical characteristics. Wobbling parameters such as trace width did not seem to influence the electrical resistance. When aluminum was the upper layer, the resistance factor was lower than in the Cu-Al configuration. This trend can be explained by keeping in mind the measured hardness values, where the hardness was much higher with copper as the upper layer. The copper-rich intermetallic compounds generated have a higher electrical resistivity, further to being hard and brittle [16]. Double welding seams resulted in a reduction in the value of k since the joint area was higher and therefore the electrical resistance lower [17]. The tested samples were the same as those reported in Table 6.

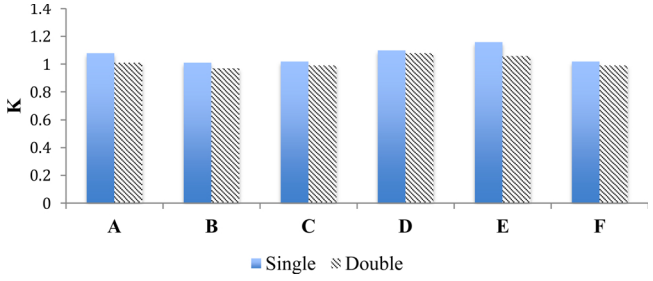

Fig. 12. Resistance factor for different samples with single and double weld seams.

4. Conclusions

Circular laser beam oscillation was applied to the welding of thin Al and Cu sheets in a lap configuration using a single mode fiber laser. To determine the properties of each weld joint, microscopy and mechanical, micro-hardness and electrical analyses were carried out. In conclusion the study can be summarized as follow:

- Wobbling amplitude greatly influences the aspect ratio of the weld seam in an Al-Cu configuration. This effect is less obvious in a Cu-Al configuration.
- Good welding seams were obtained when aluminum was on the upper side with a laser power of 600 W, a welding speed of 156 mm/s and a wobbling amplitude of 0.5 mm. With copper on the upper side, optimized parameters were a laser power of 800 W, welding speed of 134 mm/s and wobbling amplitude of 0.7 mm.
- Mechanical properties increased as the penetration depth decreased. A maximum breaking load of about 120 kgf was achieved with optimized parameters. Double weld seams involved an increase in load of about 10–20%.
- Micro-hardness testing showed an increase in hardness within fused zone. Higher values of hardness were achieved with copper on the upper side.
- Low electrical contact resistance was obtained with optimized parameters. Double weld seams represented the best configuration in this respect.
- Temperatures at 10 mm from the welding area did not exceed 45 °C. The most stressed point was close to the central area of the weld.

References

[1] Regulation (EC) No 443 of the European Parliament and of the Council. Setting emission performance standards for new passenger cars as part of the community's integrated approach to reduce CO2 emissions from light-duty vehicles 140/1-140/5 2009.

[2] Tarascon JM, Armand M. Issues and challenges facing rechargeable lithium batteries. Nature 2001;414(November (6861)):359–67. https://doi.org/10.1038/35104644.

[3] Feng, Songbai X, Wei D. Reliability studies of Cu/Al joints brazed with Zn–Al–Ce filler metals. Mater Des 2012;42:156–63. https://doi.org/10.1016/j.matdes.2012.05.028.

[4] Weigl M, Schmidt M. Modulated laser spot welding of dissimilar copper–aluminum connections. Germany: Karlsruhe; 2009.

[5] Rabkin DM, Ryabov VR, Lozovskaya AV, Dovzhenk VA. Preparation and properties of copper-aluminum intermetallic compounds. Powder Metall Met Ceram 1970;8:695–700. https://doi.org/10.1007/BF00803820.

[6] Ihor M, Schmidt M. Laser micro welding of copper and aluminum. Proceedings of SPIE – the international society for optical 2006;6107:28–33. https://doi.org/10.1117/12.648376.

[7] Akbari M, Bahemmat P, Haghpanahi M, Besharati Givi MK. Enhancing metallurgical and mechanical properties of friction stir lap welding of Al-Cu using intermediate layer. Sci Technol Weld Join 2013;18(6):518–24. https://doi.org/10.1179/1362171813Y.0000000130.

[8] Sun Z, Ion JC. Laser welding of dissimilar metal combination. J Mater Sci 1995;30:4205–14. https://doi.org/10.1007/BF00361499.

[9] Katayama S. Laser welding for manufacturing innovation. J Jpn Weld Soc 2009;78(8):682–92. https://doi.org/10.2207/jjws.78.682.

[10] Coroado J, Meco S, Williams S, Ganguly S, Quintino L, Suder W, et al. Fundamental understanding of the interaction of continuous wave laser with aluminium. Int J Adv Manuf Technol 2017;93:3165–74. https://doi.org/10.1007/s00170-017-0702-6.

[11] Smith S, Blackburn J, Gittos M, De Bono P, Hilton P. Welding of dissimilar metallic materials using a scanned laser beam. Proceedings of the 32nd international congress on applications of lasers & electro-optics (ICALEO) 2013:6–10. https://doi.org/10.2351/1.5062921.

[12] Kraetzsch M, Standfuss J, Klotzbach A, Kaspar J, Brenner B, Beyer E. Laser beam welding with high-frequency beam oscillation: welding of dissimilar materials with brilliant fiber lasers. Phys Procedia 2011;12:142–9. https://doi.org/10.1016/j.phpro.2011.03.018.

[13] Solchenbach T, Plapper P, Cai W. Electrical performance of laser braze-welded aluminum-copper interconnects. J Manuf Process 2014;16:183–9. https://doi.org/10.1016/j.jmapro.2013.12.002.

[14] Fetzer F, Jarwitz M, Stritt P, Weber R, Graf T. Fine-tuned remote laser welding of aluminum to copper with local beam oscillation. Phys Procedia 2016;83:455–62. https://doi.org/10.1016/j.phpro.2016.08.047.

[15] Zuo D, Hu S, Shen J, Xue Z. Intermediate layer characterization and fracture behaviour of laser-welded copper/aluminum metal joints. Mater Des 2014;58:357–62. https://doi.org/10.1016/j.matdes.2014.02.004.

[16] Schmalen P, Plapper P. Evaluation of laser braze-welded dissimilar Al-Cu joints. Phys Procedia 2016;83:506–14. https://doi.org/10.1016/j.phpro.2016.08.052.

[17] Schmidt P, Schweier M, Zaeh M. Joining of lithium-ion batteries using laser beam welding: electrical losses of welded aluminum and copper joints. Proceedings of the 31st international congress on applications of lasers & electro-optics (ICALEO) 2012. https://doi.org/10.2351/1.5062563.